Non-rigid Motion without Relying on Local Features: a Surface Model Applied to Vortex Tracking

Jean-Paul Berroir, Isabelle Herlin, Isaac Cohen

INRIA
INSTITUT NATIONAL DE RECHERCHE EN INFORMATIQUE ET EN AUTOMATIQUE

Non-rigid motion without relying on local features: a surface model applied to vortex tracking

Jean-Paul Berroir, Isabelle Herlin, Isaac Cohen

N° 2684

October 1995

PROGRAMME 4

ISSN 0249-6399

ROCQUENCOURT

Non-rigid motion without relying on local features: a surface model applied to vortex tracking

Jean-Paul Berroir, Isabelle Herlin, Isaac Cohen

Programme 4 — Robotique, image et vision

Projet AIR

Rapport de recherche n° 2684 — October 1995 — 24 pages

Abstract: Motion study in computer vision highly depends on the type of imagery and on the kind of the studied objects. A popular approach of non-rigid motion supposes that the objects are continuously and locally deformed. Local features, such as curvature extrema, are then often used. However, these features can not always be accurately computed, and motion may involve large deformation of the object between two consecutive temporal occurrences. In these cases, there is a real need for an approach that does not rely on local features. That study of motion requires additional information. We introduce a geometrical evolution model that enables to generate a surface interpolating the two successive contours of the object during its temporal evolution. This geometrical model may be viewed as a simplification of the true physical model of motion. This approach is particulary well suited to remote sensed data: structures of interest do not have a well defined shape, and the temporal resolution may be poor, involving large deformation. We successfully apply our model to vortex tracking on sea color images and on meteorologic images.

Key-words: Non-rigid motion, large deformation, tracking, matching, remote sensed data

(Résumé : tsvp)

Unité de recherche INRIA Rocquencourt

Domaine de Voluceau, Rocquencourt, BP 105, 78153 LE CHESNAY Cedex (France)

Téléphone : (33 1) 39 63 55 11 — Télécopie : (33 1) 39 63 53 30

Etude du nouvement non rigide sans s'appuyer sur les caractéristiques locales : un modèle de surface, appliqué au suivi de tourbillons

Résumé : L'étude du mouvement en vision par ordinateur dépend grandement de l'imagerie considérée et des objets étudiés. Dans le cas du mouvement non rigide, il est couramment supposé que les objets subissent une déformation continue et locale. L'étude du mouvement peut alors s'appuyer sur des caractéristiques locales, comme les extrema de courbure. Il est cependant possible que ces caractéristiques ne puissent être calculées avec précision, et par ailleurs que le mouvement engendre des grandes déformations de l'objet. Il y a alors un réel besoin d'étudier le mouvement, sans s'appuyer sur les caractéristiques locales, mais en introduisant un modèle d'évolution. Nous présentons un modèle géométrique d'évolution qui permet de reconstuire la surface engendrée par l'objet étudié pendant son évolution. On peut considérer ce modèle comme une simplification du véritable modèle physique du mouvement. Cette approche est bien adaptée à l'imagerie satellite : les structures d'intérêt n'ont pas de forme bien définie, et la résolution temporelle peut être faible, ce qui entraine de grandes déformations de l'objet entre deux occurences successives. Dans ce cadre, nous appliquons le modèle au suivi de tourbillons sur des images de couleur de l'océan et des images météorologiques.

Mots-clé : Mouvement non rigide, grandes déformations, suivi, mise en correspondance, imagerie satellite.

Introduction

Motion study has been formulated in various ways by computer vision specialists: application in robotics leads to the study of rigid motion; other applications, like for medical images for instance, require the study of non-rigid motion. This problem has already been widely developed. However, most approaches to non-rigid motion suppose a temporal regularity: one can assume that the studied structure undergoes a local and continuous deformation. This assumption is often called the "small deformation" hypothesis. Consequently, one can rely on local features to perform matching and tracking. A well-known approach [1, 2, 7] is actually based on curvature extrema, that are the invariants of rigid motion. Temporal regularity is also used by many authors: for instance, Geiger's [9] approach of tracking considers high curvature points of the previous frame of the tracked structure as the initialisation of the current frame. One of the characteristics of his matching approach is the search for a smooth displacement field. Serra and Berthod [17] are looking for a continuous matching function. To perform this, they minimize a criterion based on the error between the different matches, that is, the difference between translation vectors: again, temporal regularity is assumed. But this assumption may be too strong. This depends on the ratio between the velocity of the observed phenomenon and the temporal resolution of the sensor.

In the case of remote sensed data, dynamic phenomena are often observed. An interesting example is the tracking of vortex on oceanographic and meteorological images. Due to complex properties of vortex, this study can not be performed using an approach based on local features:

- A vortex is a complex structure: it is not a proper object, but a particular configuration of a fluid. It is therefore difficult to define templates such as shape or boundary. Consequently, computation of local features can not be performed accurately.

- The temporal evolution of a vortex structure involves large changes of geometry. Its topology may even vary: this may occur when two vortex interact, or when a vortex splits into two different components. Furthermore, intermediate occurrences of the temporal evolution may be missed due to atmospheric conditions: clouds prevent the acquisition of oceanographic images. Consequently, successive occurrences of the acquisition may be very different from each other.

The objective of this work is to define a model, able to perform matching of two temporal occurrences of the structure, without assuming temporal regularity, nor relying on local features.

If we can not assume the temporal regularity of motion, we have to add exogenous information to perform the matching. This information should ideally come from a physical model of the natural phenomenon; but it may be unavailable, or too heavy to be handled numerically. Therefore, we introduce a simplified model: we apply geometrical constraints to a surface interpolating the contours of two temporal occurrences of the studied structure. Such an approach presents several advantages: it enables to incorporate simplified physical constraints (as differential constraints on the surface); one can find point to point trajectories on the surface; lastly, topological changes may be handled in term of geometrical constraints (branching, pinching, ...).

The surface model is explained in section 1, while the associated geometrical constraints are explained in section 2, with different numerical methods used to compute the surface. The problems, encountered by trying to define a stable numerical scheme, lead to a simplified and efficient model definition described in section 3. At this point, the model requires adaptation to the geometry of the applicative data: in section 4 the model is then applied to a numerical simulation of the growth of a vortex, as it is observed on Coastal Zone Color Scanner (CZCS) images. Section 5 is finally devoted to the motion of a vortex on METEOSAT images.

1 Principle of modelling

In the context of motion involving large deformation, the tracking of a structure, without any knowledge of its geometry and motion, has no sense. It is fundamental to design a model adapted to that knowledge. In this section, we explain the principle of such an approach. The adaptation of the model to specific applicative structures is the subject of following sections. However, we restrict this discussion to the case of planar structures represented by their boundaries.

We suppose we are given two temporal occurrences of the structure, namely, two 2D boundaries. The evolution of the structure between these occurrences generates a continuous 3D surface, with the third dimension being time. The main objective is to compute the best possible surface. To perform this task, we require an evolution model, expressed as constraints applied to this surface. The problem is then to find the surface interpolating the two contours and respecting these constraints.

This formalism presents several advantages:

- It is possible to incorporate information about the physical model of temporal evolution, by expressing it as differential constraints applied to the surface. When it is not possible or too difficult, it is necessary to design geometrical constraints. The corresponding evolution model,

based on the geometrical constraints, can then be considered as a simplification of the true physical model of evolution.

- Intermediate occurrences of the contour may be retrieved: they are cross sections of the surface, parallel to the original contours. This is the justification of this approach: the surface carries information about the evolution model of the structure and therefore enables the retrieval of the continuous evolution of the structure between two given temporal occurrences. The surface is in fact only constrained by the evolution model, not by local features of the contours.

- Point trajectories are included in the surface. It is possible to compute them, using the Hamilton-Jacobi formalism for instance.

- Topological changes may be expressed using geometrical considerations. Figure 1 illustrates this property with the example of a structure splitting from one connected component into two different components. This can be modelled in term of branching.

These last two properties are in fact the subject of future studies and will not be discussed in details in this paper.

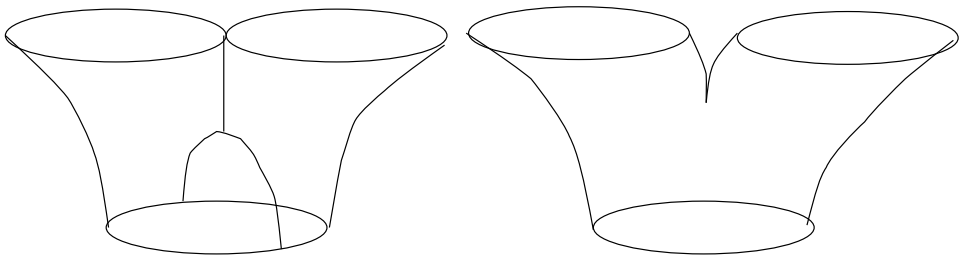

Figure 1: Examples of an interpolating surface with change of topology.

2 Definition of the surface model

We have already mentioned that the model is based on geometrical constraints. In order to obtain a smooth temporal evolution, an elastic behavior is imposed to the surface. The purpose of this section is to explicitly define the evolution model and to propose a direct implementation.

We are given two 2D contours C_1 and C_2 placed in two parallel planes $z = t_1$ and $z = t_2$, t_i being the date of acquisition of the contour C_i. Since the model only deals with two dates, the temporal axis has an arbitrary scale. Assuming that $t_1 = 0$ and $t_2 = 1$ does not influence further computation. In order to focus this study on deformation, we first apply the rigid motion that performs the best matching between the two contours C_1 and C_2. This enables to manage the global translation motion that is often observed on meteorological and oceanographic image sequences. We then look for an interpolating surface ϕ, with an elastic behavior, containing C_1 and C_2. The surface ϕ is described by two parameters $(s, r) \in \Omega = [0, 1]^2$. The parameter r represents in fact the time. A constant value of r generates a cross section of the surface parallel to the original contours and described by s. The intermediate temporal occurrences of the contour are then described by the different values of r between 0 and 1.

Elasticity may be modelled by control of the first fundamental form. This form, $\mathcal{F}$ (see equation 1, where $< .,. >$ is the dot product in $\mathbb{R}^3$), expresses the distortion produced by ϕ on an elementary square of the parameters' space.

$$\mathcal{F} = \begin{pmatrix} < \frac{\partial \phi}{\partial s}, \frac{\partial \phi}{\partial s} > & < \frac{\partial \phi}{\partial s}, \frac{\partial \phi}{\partial r} > \\ < \frac{\partial \phi}{\partial s}, \frac{\partial \phi}{\partial r} > & < \frac{\partial \phi}{\partial r}, \frac{\partial \phi}{\partial r} > \end{pmatrix} \tag{1}$$

If $\mathcal{F}$ is equal to identity, the local basis $(\frac{\partial \phi}{\partial s}, \frac{\partial \phi}{\partial r})$ of the tangent plane of ϕ is orthonormal. In this case the distortion is minimal. Moreover, the closer to identity is $\mathcal{F}$, the smaller is the distortion. We then measure the local distortion of the surface by the expression (2), where Id stands for identity matrix:

$$||\mathcal{F} - Id||^2 \tag{2}$$

The elastic behavior is obtained by minimizing the integral of this criterion over the surface. This corresponds to the following energy functional:

$$E(\phi) = \int\int_{\Omega} \left((< \phi_s, \phi_s > -1)^2 + 2 < \phi_s, \phi_r >^2 + (< \phi_r, \phi_r > -1)^2 \right) dsdr \tag{3}$$

Minima of $E(\phi)$ are solutions of $\nabla E(\phi) = 0$; this leads to the following differential system (where ∇^T stands for the transposate of the gradient operator):

$$\triangle \phi - \nabla^T(\mathcal{F} \nabla \phi) = 0 \tag{4}$$

This equation expresses the evolution model. The surface must also verify boundary conditions. Because the surface, that we are looking for, interpolates the two original contours, we obtain the

two following boundary conditions concerning $r = 0$ and $r = 1$: $\phi(.,0) = C_1$ and $\phi(.,1) = C_2$. Conditions concerning $s = 0$ and $s = 1$ depend on the topology of the contours. We previously mentioned that topological changes are not discussed in this paper. This study is restricted to the case where the two contours have only one connected component. If the contours are closed, the surface has then the topology of a cylinder, and the boundary conditions are those of equation (5). If they are opened, with no more information, we do not apply constraints on $s = 0$ and $s = 1$.

$$\begin{cases} \phi(.,0) = C_1 \\ \phi(.,1) = C_2 \\ \phi(0,.) = \phi(1,.) \end{cases} \tag{5}$$

The energy is of course not quadratic. To achieve numerical resolution, we use a relaxation model (eq. 6):

$$\frac{\partial \phi}{\partial \tau} + \triangle \phi - \nabla^T(\mathcal{F} \nabla \phi) = 0 \tag{6}$$

where τ is the relaxation time of the system. After discretization and linearization of equation 6, ϕ at time $\tau + d\tau$ may be computed knowing ϕ at time τ. We therefore need an initial estimate, ϕ at time $\tau = 0$, that can be a bilinear interpolation of the two contours. Moreover, ϕ must be forced, at each step of the relaxation process, to respect the boundary conditions.

This process has the advantage of being easy to implement. It is a direct implementation of the evolution model. It has yet several drawbacks:

- As the energy functional is not convex, each solution is in fact associated to the initial estimate. It is therefore crucial to find a sufficiently good estimate of the surface.

- Getting the first fundamental form close to identity tends to produce parallel cross sections of length 1. But the lengths of the original contours (L_1 for C_1 and L_2 for C_2) are given and that of the cross section must vary along the r-axis between these two values. This can be easily solved by minimizing the norm of $\mathcal{F} - K(r)$ where $K(r)$ is:

$$K(r) = \begin{pmatrix} rL_2 + (1-r)L_1 & 0 \\ 0 & 1 \end{pmatrix} \tag{7}$$

  Remaining calculation is unchanged. This scheme tends to make the length of the cross sections vary linearly between L_1 and L_2.

- The most important problem concerns regularity. We saw that we must force the surface to respect the boundary conditions during the relaxation process. Irregularities may occur on the

surface near the two original contours. Furthermore, the energy functional does not prevent local discontinuities. Therefore, the regularity of the surface is not assured.

Acting on regularity can be performed by adding a new criterion: for instance it is possible to minimize the integrate of the norm of the gradient $(\frac{\partial \phi}{\partial s}, \frac{\partial \phi}{\partial r})$ over the surface, like for the usual internal energy of "snakes". But combining two types of antagonist criteria (namely, the elasticity criterion based on the first fundamental form and the internal energy of snakes) supposes to adjust the weighting coefficients of the associated energies. It seems difficult to find them automatically. The regularity is even not assured: the optimum is a compromise between the two criteria.

A regular surface can be obtained by using the snake formalism only, and therefore by leaving the former definition of the energy functional (eq. 3). The idea is to combine the internal energy of snakes with a criterion that forces the surface to interpolate the two original contours. The problem is that the internal energy of snakes does not provide an evolution model: it only has a smoothing effect. It does not provide the information needed to reconstruct the motion. These reasons lead us to design a more constrained model.

3 Constrained model

The problem is now to combine the criteria based on the first fundamental form and on the regularity of the surface. A simple method to obtain a regular surface is to restrict the space of available surfaces. In other words, we try to define a parametric model of the surface. We decide to consider the bilinear interpolations of the two contours as the set of available surfaces.

More accurately, if the contours are described by their curvilign abscissa, a bilinear interpolation is generated by a function f, that links the curvilign abscissa of the two contours. If the lengths of the two opened contours C_1 and C_2 are respectively L_1 and L_2, each function f mapping $[0, L_1]$ into $[0, L_2]$ generates the following bilinear interpolation (see eq. 8):

$$S(s,r) = \begin{cases} x(s,r) &= (1-r)x_1(s) + rx_2(f(s)) \\ y(s,r) &= (1-r)y_1(s) + ry_2(f(s)) \\ z(s,r) &= r \end{cases} \tag{8}$$

where $s \in [0, L_1]$, $r \in [0, 1]$ and $(x_i(s), y_i(s))$ is the point of contour C_i with curvilign abscissa s. This equation also stands in the case of closed contours, but one first has to determine the origin of the curvilign abscissa of the two contours. However, as the application concerns vortex tracking, which are represented by opened contours, this problem is not discussed in this paper.

The set of available surfaces is too restricted for us to compute realistic point trajectories. But it enables a simple formulation of the matching between two contours: the pairs of matched points are those of curvilign abscissa s and $f(s)$ respectively. The computation of the energy functional (equation 3) also gets easier: first, we are now looking for the matching function f, which is a one-dimensional problem; then, integrating the energy functional along the r-axis can be approximated by the area of a quadrangle (see figure 2, where X_1 and X_2 are a pair of matched points with curvilign abscissa s and $f(s)$, $\vec{\Gamma_i}$ is the tangent of C_i at X_i with norm 1). We compute this area

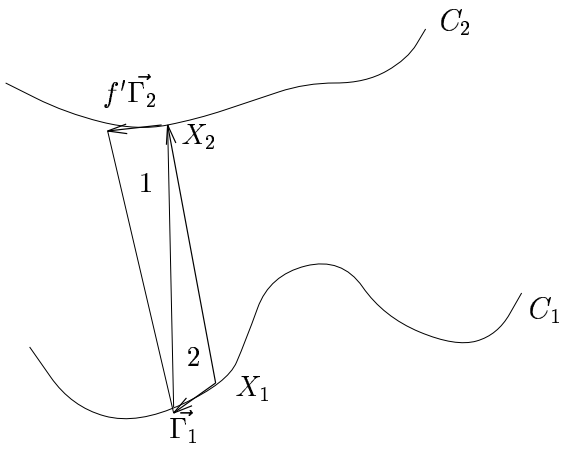

Figure 2: Matching criterion

as the summation of the two triangles numbered by 1 and 2 on figure 2. The associated energy is defined by:

$$e(f) = \int_s (\overrightarrow{X_1X_2(f)} \wedge \overrightarrow{\Gamma_1})^2 + (\overrightarrow{X_1X_2(f)} \wedge f'\overrightarrow{\Gamma_2(f)} + f'\overrightarrow{\Gamma_2(f)} \wedge \overrightarrow{\Gamma_1})^2 \tag{9}$$

One can compute the gradient of this functional to obtain the following differential equation (where $\overrightarrow{\Gamma_i}$ and $\overrightarrow{N_i}$ are the normalized tangent and normal vectors of the contour C_i):

$$\begin{aligned} &< \overrightarrow{X_1X_2(f)} \wedge \overrightarrow{\Gamma_1}, \overrightarrow{\Gamma_1} \wedge \overrightarrow{\Gamma_2(f)} > + f''(\overrightarrow{X_1X_2(f)} - \overrightarrow{\Gamma_1}) \wedge \overrightarrow{\Gamma_2(f)})^2 + \\ &f'^2 < (\overrightarrow{X_1X_2(f)} - \overrightarrow{\Gamma_1}) \wedge \overrightarrow{\Gamma_2(f)}, (\overrightarrow{X_1X_2(f)} - \overrightarrow{\Gamma_1}) \wedge \overrightarrow{N_2(f)} > \quad = 0 \end{aligned} \tag{10}$$

It is now possible to perform the matching of the two temporal occurrences of the structure by solving this one-dimensional differential equation (eq. 10). However, the energy functional may still be non convex, and does not prevent local discontinuities. This equation could be solved by a gradient descent method, but we would not be sure to obtain neither a regular solution, nor a mapping of the two contours: the matching function has to realize a mapping from $[0, L_1]$ into $[0, L_2]$

and therefore has to be non decreasing. This is not assured by a gradient descent. Another difficulty is to avoid local minima of the energy. This is the reason why we chosed to use a parametric model for the matching function. It is important to design this model accordingly to the geometry of the structure. We would then be assured of finding a regular and non decreasing function, able to perform an efficient matching of the two boundaries.

Designing this parametric model constitutes the adaptation of the global approach to the specific applicative structure we are studying. The basic idea is to roughly decompose the structure into meaningful regions. This decomposition does not need to be accurate: it is just necessary to point out parts of the boundaries that have to be matched. Let us now suppose that we distinguish n meaningful segments on the structure. To match them on two temporal occurrences, we have to find $(n-1)$ couples of matched points, that correspond to the limits of these regions on each of the two contours. These $(n-1)$ key points are defined by $(n-1)$ values s_i of the curvilign abscissa of the first contour, and $(n-1)$ corresponding values $f(s_i)$. The matching function has to be approximately linear on each of these regions. A simple solution would be to look for a piecewise linear function interpolating the $n-1$ key points and the two additional ending points $(0,0)$ and (L_1, L_2). In order to obtain a sufficient regularity, we perform a $\mathcal{C}^2$ smoothing of the piecewise linear function. Seeking the matching function is then equivalent to finding the $(n-1)$ key points.

It is of course difficult to obtain an expression of the energy and its gradient as a function of the key points. But the fact that the function has to be non decreasing reduces the search space. A hierarchical minimization process can be used to find the solution: the possible values of the key points depend on the discretization of the intervals $[0, L_1]$ and $[0, L_2]$. The idea is to start from a rough discretization (namely, 20 possible values for each interval) and to progressively refine the discretization. Initial key points are the ones that realize the minimum of the energy (eq 9) among the initial possible values. At each step, the discretization is refined, and the set of possible values of the key points is reduced by the fact that the piecewise linear function interpolating them is non decreasing. Provided that the initial discretization was thin enough to avoid a local minimum, the algorithm converges with a reasonable computational cost: for instance, on oceanographic images, performing the matching of two occurrences of a vortex, that is divided into five regions, takes approximately 20 seconds of user time on a DEC-Alpha work station (each occurrence of the boundary being represented by approximately 600 points).

4 Vortex tracking on oceanographic images

As previously mentioned, classical approaches of non-rigid motion may not be adapted to remote sensed data. There are two main reasons:

- the observed structures are often not related to a physical object, but they express physical measurements of fluids: meteorologic images measure the water vapor density in the atmosphere, oceanographic images may for example concern the temperature of the sea. A vortex is a specific configuration of the fluid in motion. Thus, it is uneasy to define its shape and its boundary. As a consequence, one can not expect to compute local features accurately. It is in particular the case for curvature (and a fortiori curvature extrema) measure, the definition of which involves differential characteristics of order 2.
- The temporal resolution of the sensor is related to the trajectory of the satellite, to the time it spends to perform an acquisition, and to atmospheric conditions. In the case of oceanography, temperature measurement can not be done under any atmospheric conditions: clouds prevent the acquisition of AVHRR images (infra-red measurements) and of CZCS images (color measurements). It is therefore possible to miss several occurrences of the vortex evolution.

This section is devoted to the application of the model to vortex tracking on oceanographic images. We will first describe the static model of vortex, and the characteristics of vortex motion. We will then show results on a numerical simulation of the growth of a vortex.

4.1 Vortex on oceanographic images

Measurements of the sea surface can be done by several sensors: AVHRR (Advanced Very High Resolution Radiometer) images provide direct temperature measures (infra-red signal), and CZCS (Coastal Zone Color Scanner) provides information about the color of the sea, which is somehow related to temperature. Figure 3 displays the same vortex on CZCS and AVHRR images. This vortex presents the typical "mushroom" like shape. Such a structure may be modelled by two rolls and an arc delimiting its expansion: on figure 4, three steps of the evolution of the vortex of figure 3 are displayed, together with the result of their static modelling. This detection is performed automatically (see [11, 12] for details on vortex modelling and detection on CZCS images). This static model provides both geometrical and quantitative information on the vortex. During its evolution, the two rolls expand and have an approximately constant mean position, regardless of

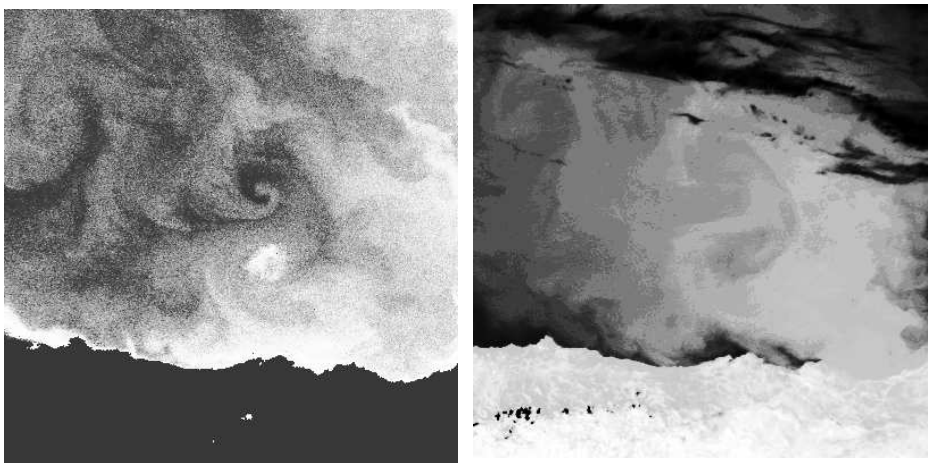

Figure 3: The same vortex on a CZCS (left) and AVHRR image (right). (Courtesy of ACRI firm and OCEAN european project).

Figure 4: Three steps of vortex evolution on a CZCS temporal sequence, and their static model (data provided by ACRI firm and OCEAN european project).

the global translation involving the whole structure. The external boundary also expands in a constant direction.

The vortex on figure 4 is fully developed. A more interesting part of its evolution is the beginning of its growth: starting from a straight line (a temperature front), the vortex progressively builds up, and finally reaches the typical mushroom like shape. Figure 5 illustrates this process: it is a numerical simulation of the growth of a vortex. One can remark that the beginning of evolution is fast. Therefore, the early steps of evolution are observed with a poor temporal resolution. The observation of all the steps of figure 5 on natural images is actually very rare and difficult. Obviously, there is a need for matching a vortex at the beginning of its evolution with a fully developed "mushroom like" vortex; this can not be done with an approach based on curvature extrema. The reason is that some parts of the vortex are hardly perceptible in the early steps: the number of curvature extrema increases during the evolution, as the mushroom shape becomes visible.

4.2 Results

To apply the matching model, we need to extract a contour representation of the vortex, and to separate it into meaningful regions. A contour can be derived from the static model of vortex and has the same shape as that of the numerical simulation of figure 5. However, the results displayed in this section are computed on the simulation. This sequence is made of nine 260×260 pixels images. It has the advantage that we can study the behavior of the matching model with near temporal occurrences, when the small deformation hypothesis holds, and also with realistic cases, when it does not. Contours extraction is done using standard image processing tools and we obtain a regular representation by fitting the contour with a non uniform B-spline of order 7. This provides a good estimate of curvature. We then discretize each contour into approximately 600 values of curvilign abscissa.

The separation of the fully developed vortex into meaningful regions is based on its static representation. We distinguish five regions that are displayed and numbered on figure 6: the region 3 is the arc that delimitates the expansion of the vortex, the regions 2 and 4 are the inner boundaries of the two rolls, and the regions 1 and 5 are the front line on which the vortex appears. These five regions define four key points. Again, we insist on the fact that this segmentation does not need to be precise. The important point is to distinguish what are the meaningful segments of the structure. The fact, that the separation points approximately correspond to curvature extrema on figure 6,

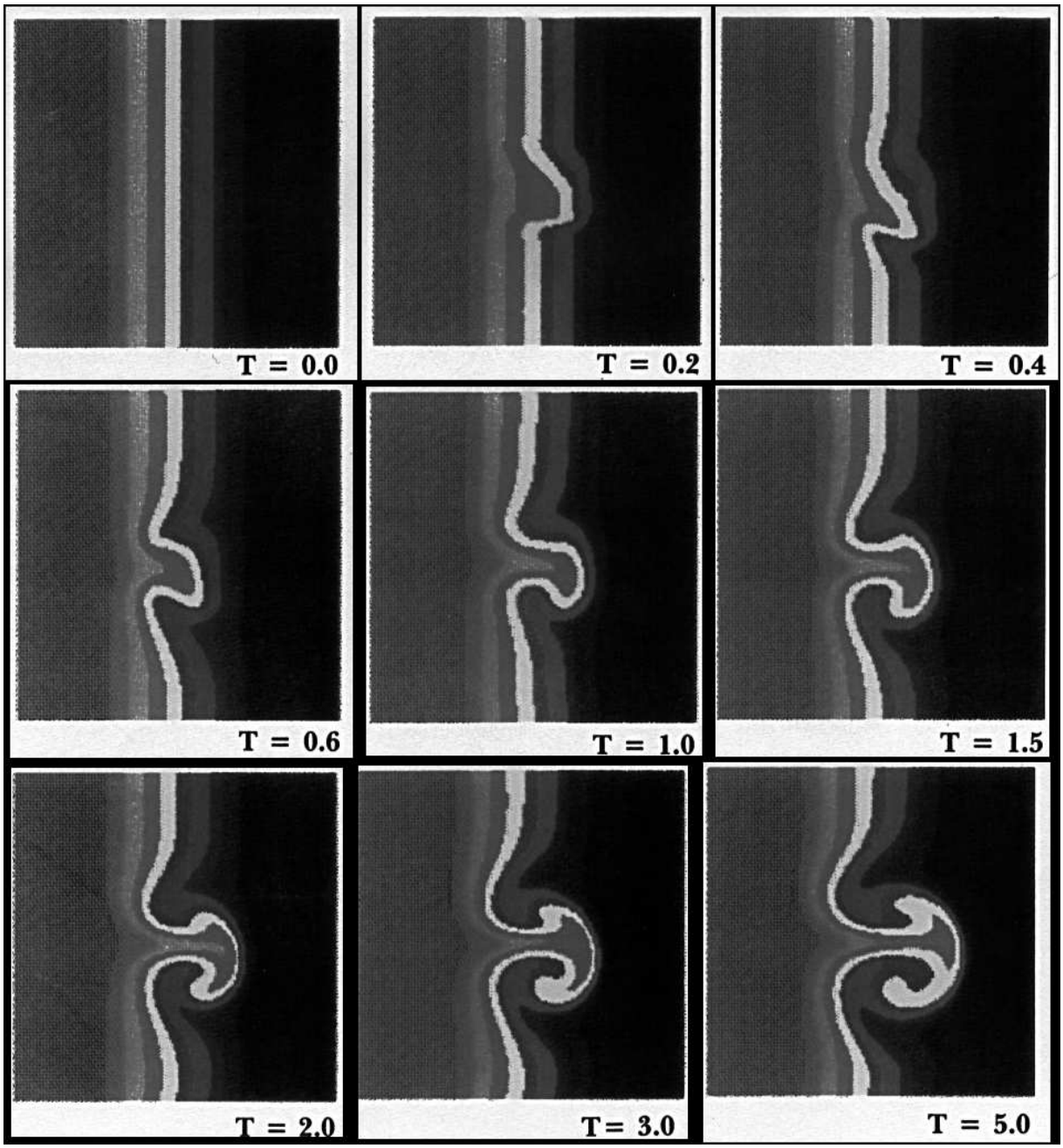

Figure 5: Numerical simulation of vortex evolution (provided by EOS).

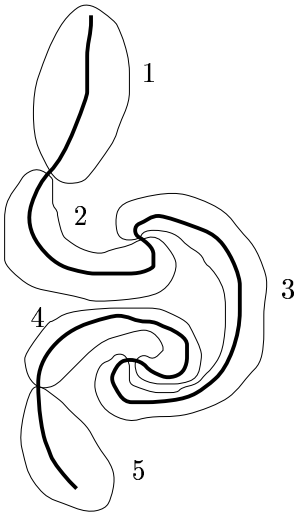

Figure 6: Decomposition of a vortex contour into five meaningful regions.

does not mean that we could have based our approach on them. One has to keep in mind that these regions do not grow at the same time and speed. Thus, curvature extrema do not necessarily separate those regions at each step of evolution.

We first have to validate the matching model, because it has to behave properly when the small deformation hypothesis holds: validation consists in verifying that the regions defined on figure 6 are matched, and mostly in checking wether curvature extrema, which are relevant features in this case, are coorectly matched. The corresponding result is shown on figure 7: we have performed the matching between the successive temporal occurrences of the simulated sequence of figure 5, which slightly differ from each other. We check that the matching is correctly performed. In this case, although curvature is not used in the model, curvature extrema are matched: figure 9 illustrates this point. It is the plot of the curvature of contour C_1 at curvilign abscissa s and curvature of C_2 at curvilign abscissa $f(s)$. The four curvature extrema (two positive and two negative) are exactly matched.

To validate our model in the general case, we performed the matching between the early steps of the temporal evolution and the fully developped vortex. All the regions we have defined on figure 6 are not developped at the beginning of evolution. This is in particular the case of the two rolls. As we can not expect curvature extrema to be relevant, the validation only consists in checking wether the perceptible regions are matched with their corresponding ones on the fully developped

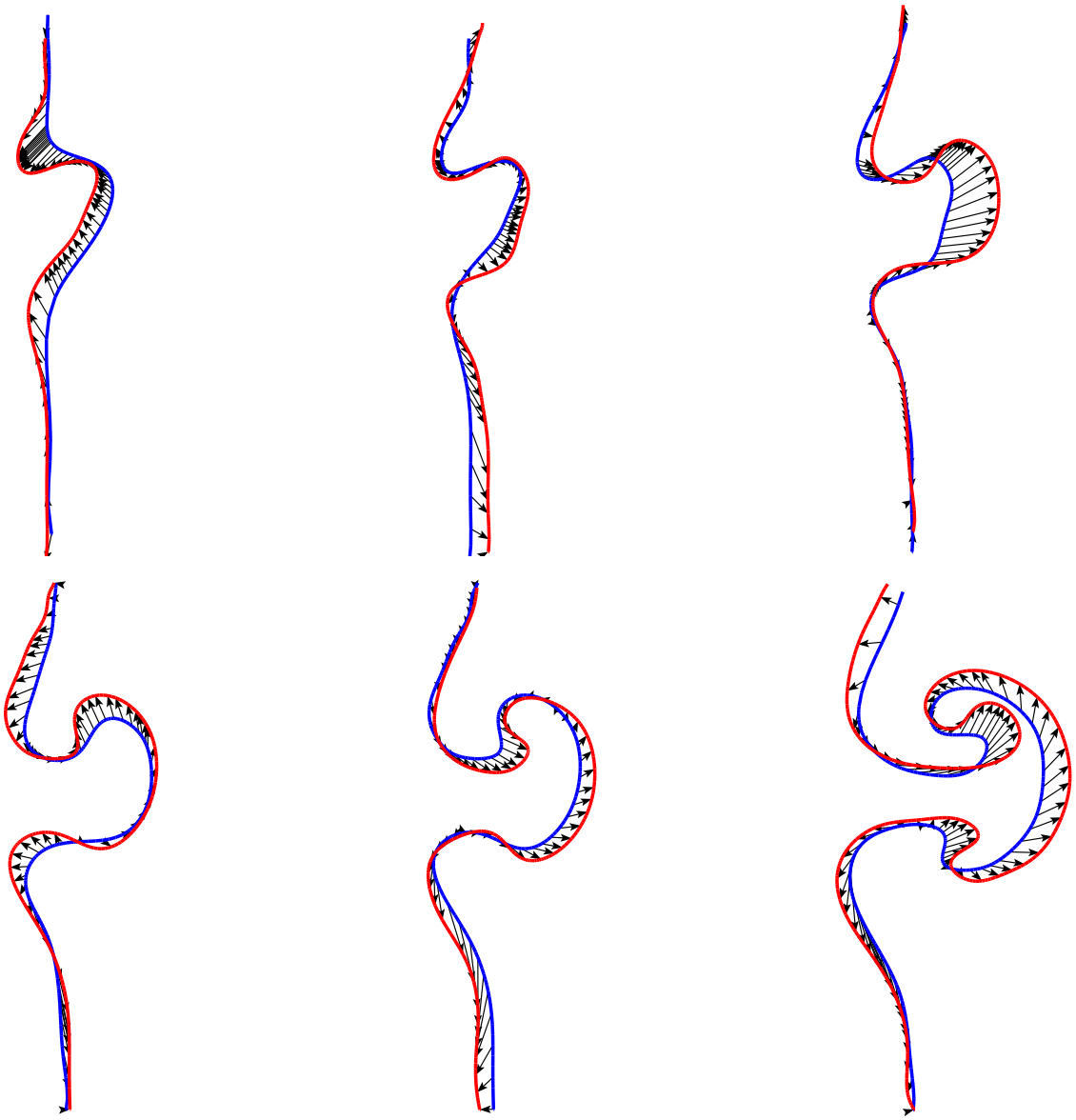

Figure 7: Tracking of the vortex during its evolution, with thin temporal resolution.

vortex. This can be verified on figure 8, which displays the matching between the occurrences 2 to 6 of the simulated sequence and the last one. As expected, curvature extrema are no more

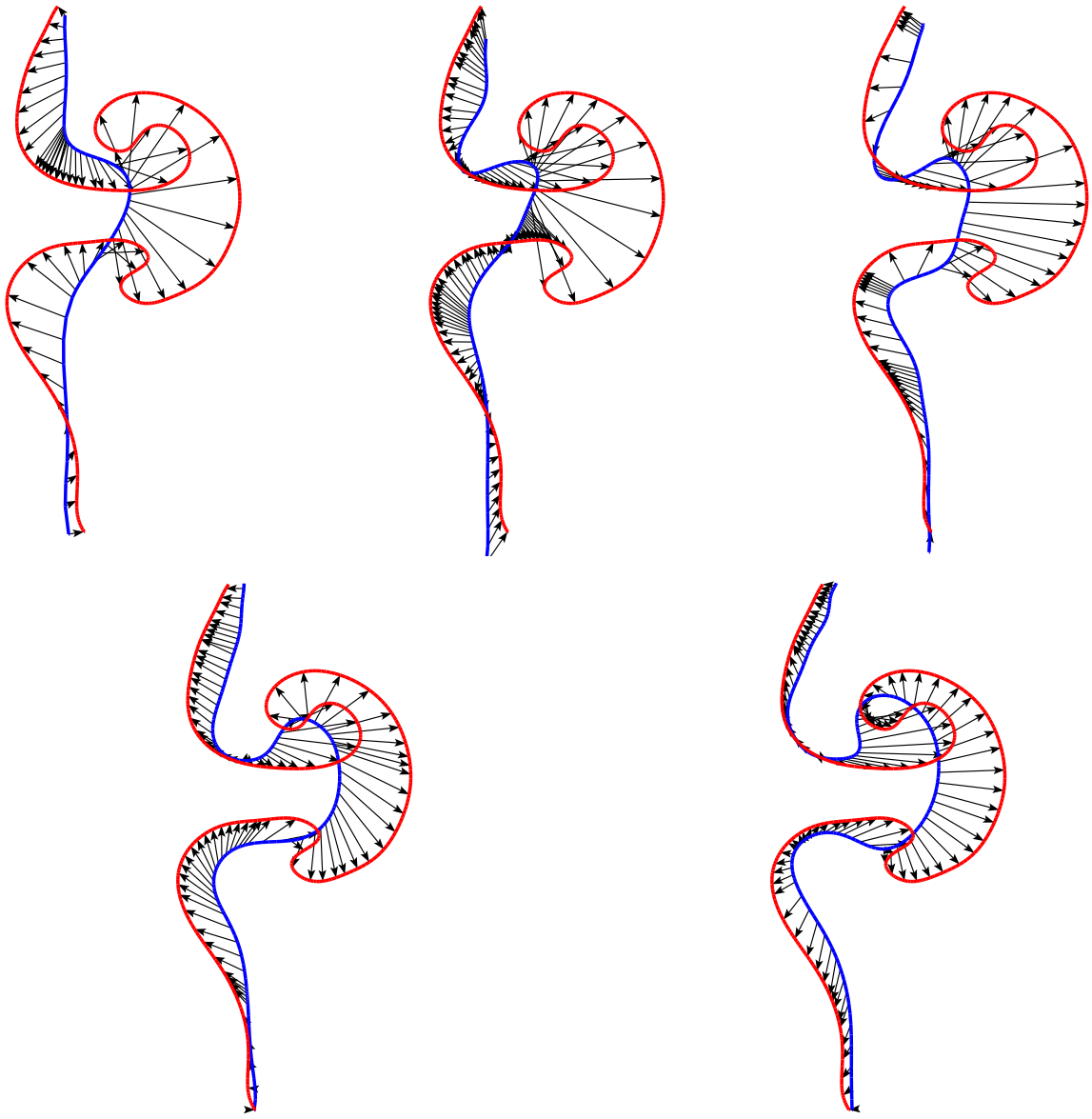

Figure 8: Matching of early occurrences of the vortex with the last occurrence. Small deformation hypothesis does not hold anymore.

relevant features. More precisely, it is the case of the two negative extrema, which correspond to the rolls, because these regions are actually hardly perceptible on the early steps of evolution. The two positive curvature extrema, which correspond to the limits of the arc, are exactly matched,

because this region is visible on each of the images. Figure 10 illustrates this point for the matching between the fourth and the last image of the sequence.

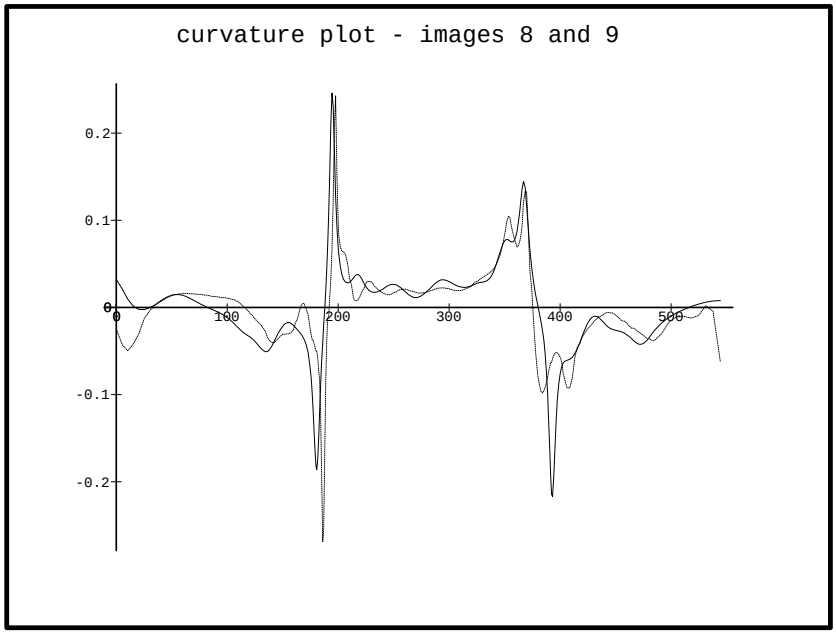

Figure 9: Curvature plot of the matching between images 8 and 9 of the simulated sequence. Curvature extrema are correctly matched.

5 Vortex tracking on meteorological images

METEOSAT images measure the temperature and the water vapor density of the atmosphere. This information is related to the presence of clouds. Therefore, vortex are commonly observed on these images. This section is devoted to the application of the matching model to a sequence of METEOSAT temperature (infra-red) images. We first present the static model of the vortex and the characteristics of its motion. This leads to the adaptation of the matching model to the vortex structure. We then present the results obtained on the sequence.

5.1 Vortex modelling and motion

A vortex observed on METEOSAT images does not have the same structure as on oceanographic images: on figure 11 is displayed the temperature and the water vapor density of the same vortex structure. It presents a single roll, while the vortex studied on oceanographic images are made of two

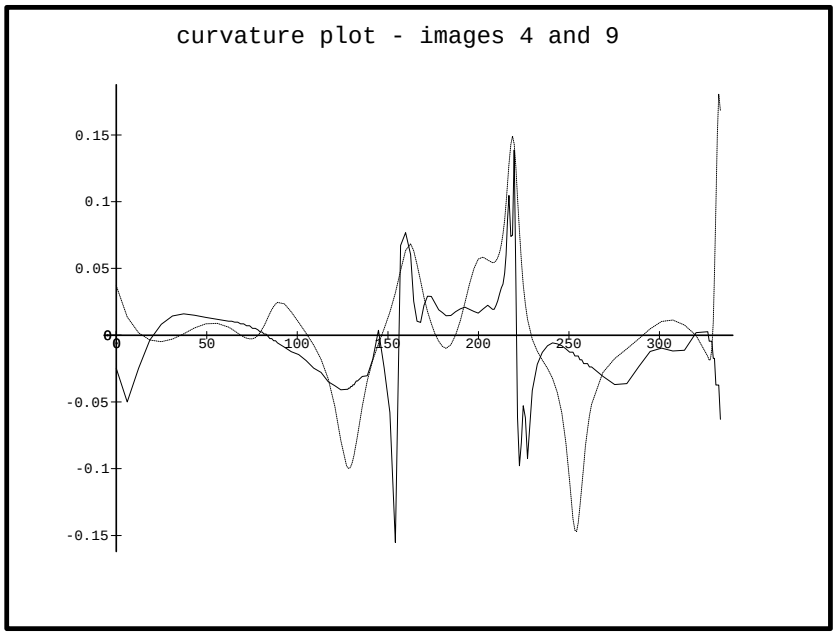

Figure 10: Curvature plot of the matching between images 4 and 9 of the simulated sequence. Negative curvature extrema are not matched.

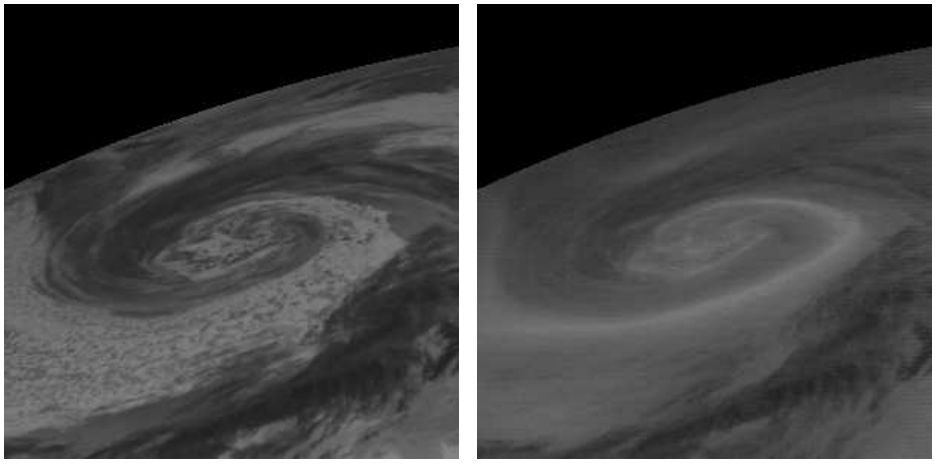

Figure 11: Temperature (left) and water vapor density (right) measure of the same vortex structure on a METEOSAT image.

rolls rotating in opposite directions. One can distinguish several bands of homogenous temperature winding around the vortex's center. We have chosen to model the vortex by its brightest band. Detection is performed using snake modelling. On figure 12 is displayed some occurrences of a vortex and their static model. Regardless of a global translation motion, the vortex radially expands

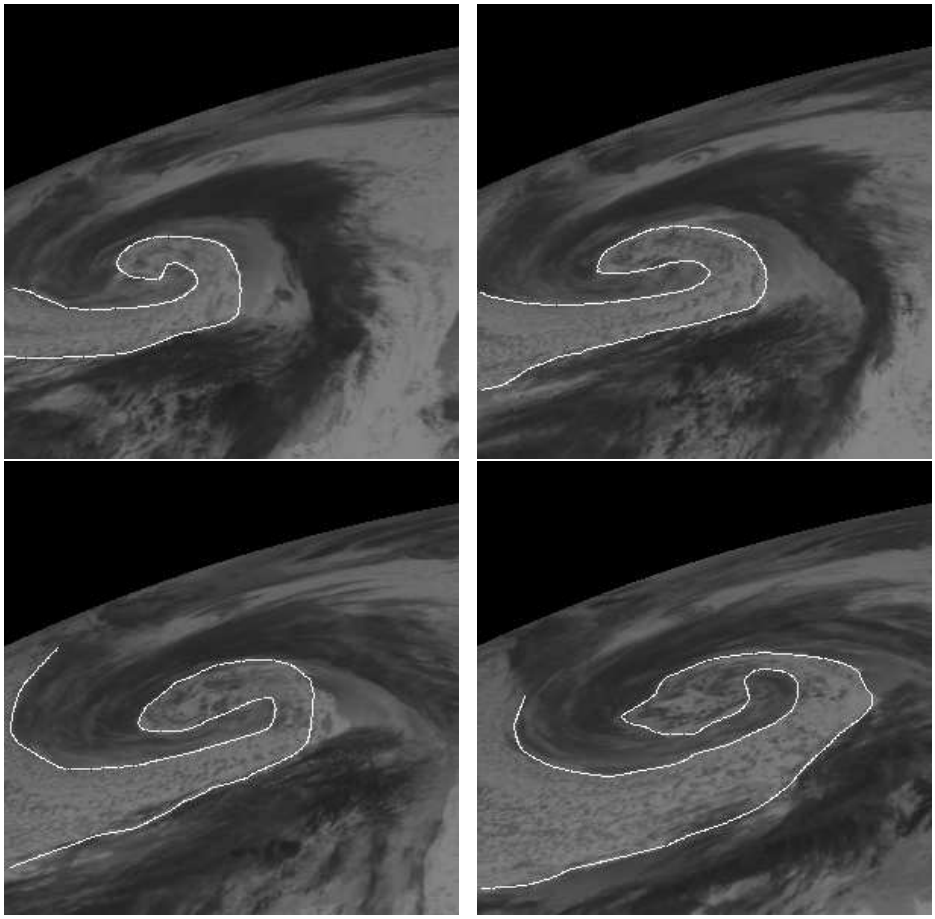

Figure 12: Four occurrences of a vortex on a METEOSAT temperature sequence, together with their segmentation.

and has a rotation motion around its center. The separation of the vortex into meaningful regions is performed as for oceanographic images: we distinguish the roll and the limits of the band. This constitutes three regions. We are then looking for two key points.

5.2 Results

The original sequence is made of 48 images of size 950×450 pixels that cover approximately the fourth part of the earth surface. We have extracted seven small images of size 300×300 centered on a

vortex. These images are regularily spaced from the 30^{th} to the last image of the original sequence. As previously, we first validate the model on cases where the small deformation hypothesis is valid. The corresponding result is shown on figure 13, where are displayed the matching between successive frames of the extracted sequence. The curvature plot on figure 15 allows to check that the curvature extrema are matched. The model also behaves well in the large deformation case: this is illustrated on figure 14, where are displayed the matching between early frames of the sequence with the last one. Again, one can check that curvature extrema are not matched anymore: see the curvature plot on figure 16.

6 Conclusion

Modelling deformation is a crucial problem when studying motion. Large deformation often occur with remote sensed data, and more generally with applications concerning environment. Our approach to this problem is to impose a geometrical model of evolution when the physical model is not available. That model allows tracking and matching of natural structures without relying on local features. It is designed according to the geometry of the structure but can easily be adapted to other kind of structures.

Several improvements are possible. First, we have restricted the set of surfaces to bilinear interpolations. Consequently, point to point trajectories are included in a straight line: we only perform matching. Finding realistic trajectories supposes to use a larger class of surface. Introducing an evolution model, that is closer to the physical one, could help restricting the surface class in an appropriate way. At last, this approach, based on a parameterization of the contours, supposes an a priori known topology. Handling topological changes requires further research.

Acknowledgements

CZCS images are provided by OCEAN european project. We thank ACRI company for providing oceanic structures description on these data. We are grateful to A. Szantaï and M. Desbois from the Laboratoire de Météorologie Dynamique (LMD, Ecole Polytechnique, France) for having provided us METEOSAT images.

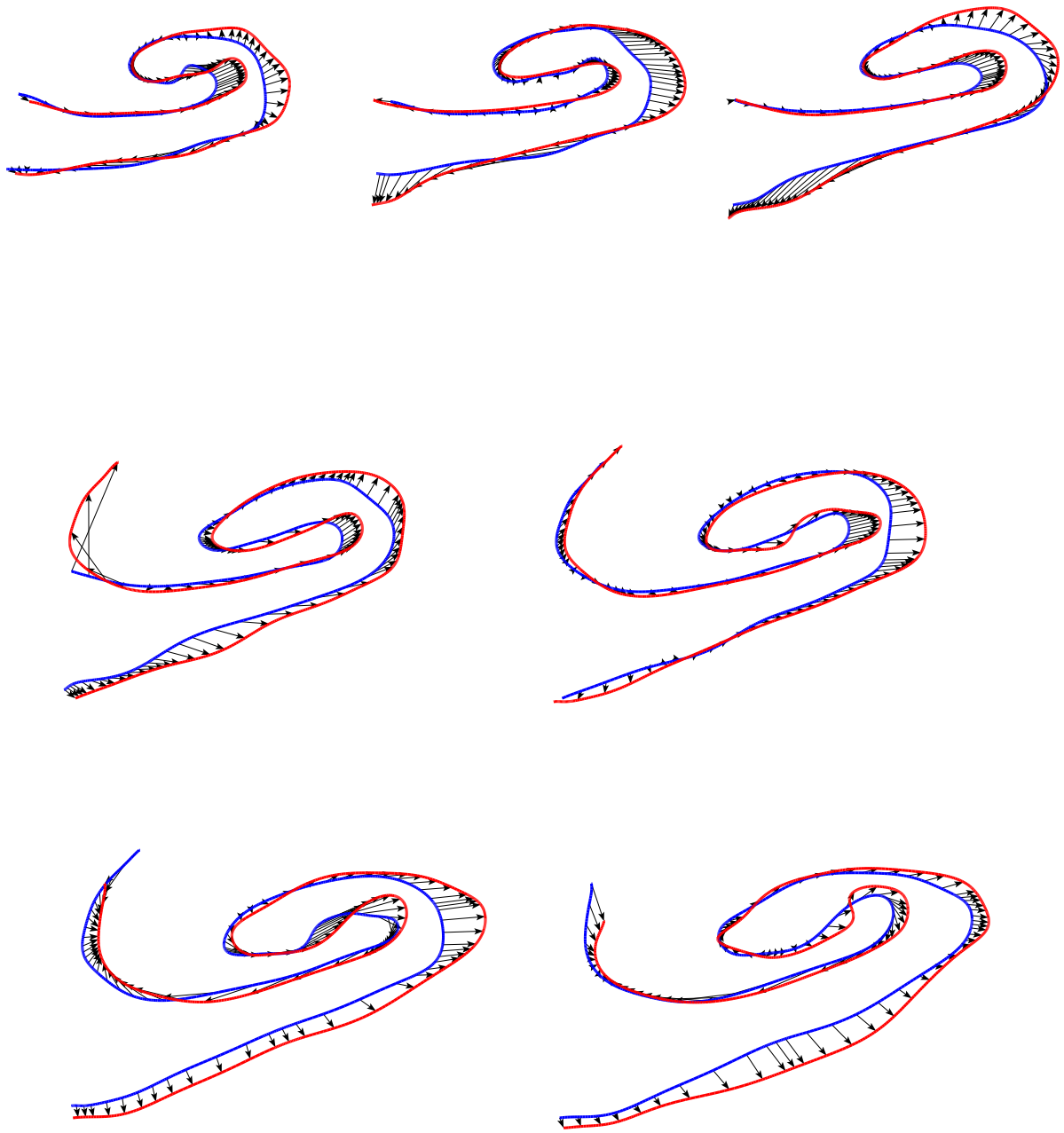

Figure 13: Tracking of the vortex during its evolution, with thin temporal resolution.

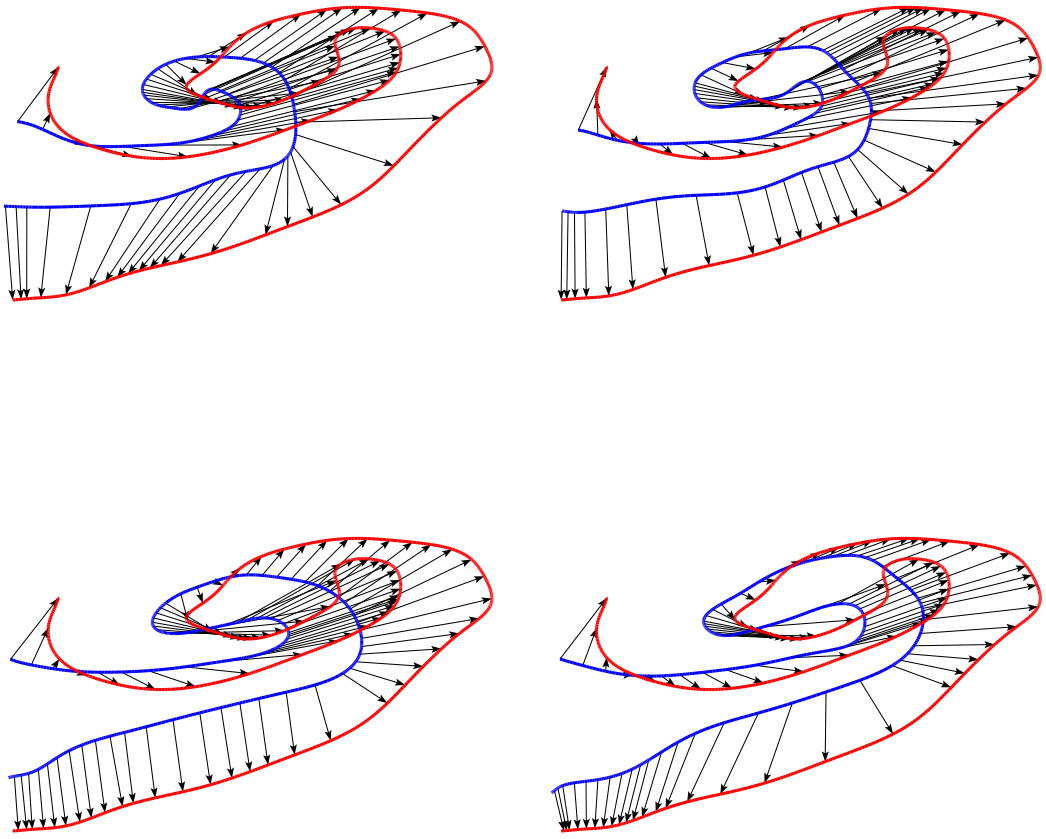

Figure 14: Matching of early occurrences of the vortex with the last one. Small deformation hypothesis does not hold.

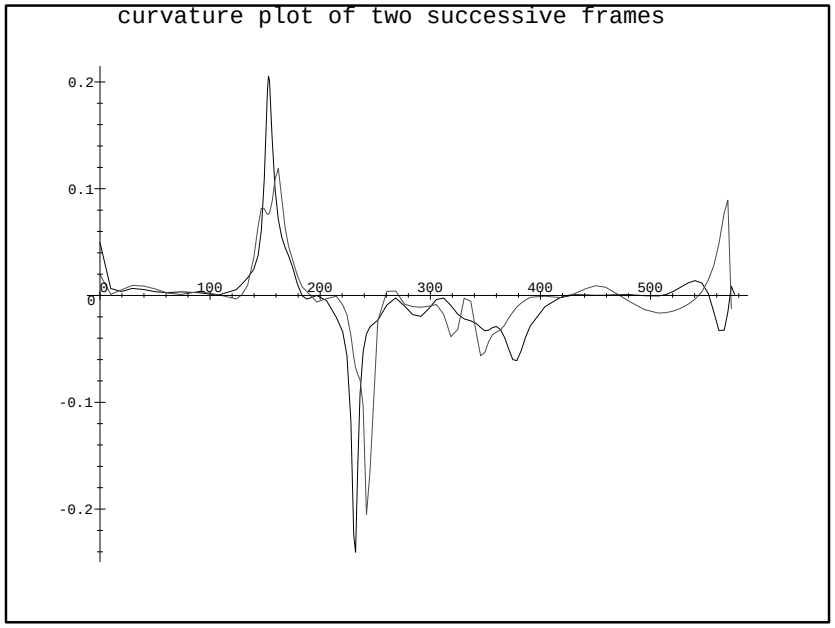

Figure 15: Curvature plot of two successive frames of the sequence; curvature extrema are matched.

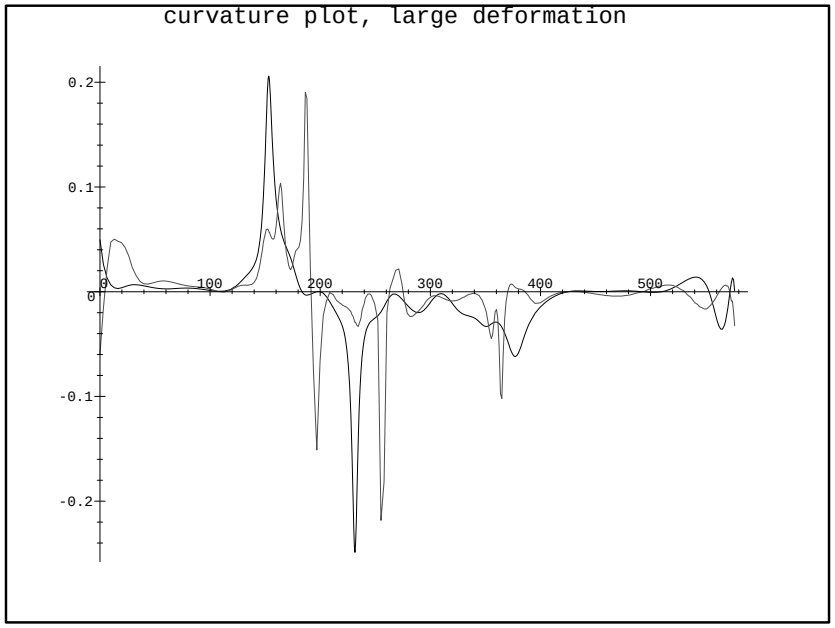

Figure 16: Curvature plot of two distant frames of the sequence; curvature extrema are not matched.

References

[1] A.A. Amini, R.L. Owen, and J.S. Duncan. Non-rigid motion for tracking left-ventrical wall. In *IPMI*, 1992.

[2] N. Ayache, I. Cohen, and I.L. Herlin. Medical image tracking. In Andrew Blake and Alan Yuille, editors, *Active Vision*, chapter 17. MIT Press, Cambridge, Mass, 1992. December.

[3] I.A. Bachelder and S. Ullman. Contour matching using local affine transformations. In *Image Understanding Workshop*, Jan 1992.

[4] J.P. Berroir, S. Bouzidi, I.L. Herlin, and I. Cohen. Vortex segmentation on satellite oceanographic images. In *SPIE Satellite Remote Sensing*, Rome, September 1994.

[5] J.P. Berroir, I.L. Herlin, and I. Cohen. Tracking highly deformable structures: a surface model applied to vortex evolution within satellite oceanograph ic images. In *EOS-SPIE Satellite Remote Sensing II*, 1995.

[6] A. Blake and R. Cipollo. The dynamic analysis of apparent contours. In *1st European Conference on Computer Vision*, Antibes, France, 1990.

[7] I. Cohen, N. Ayache, and P. Sulger. Tracking points on deformable objects using curvature extrema. In *European Conference on Computer Vision*, Santa Margherita Ligure, Italy, May 1992.

[8] J.S. Duncan, R.L. Owen, L.H. Staib, and P. Anandan. Measurement of non-rigid motion using contour shape descriptors. In *Computer Vision and Pattern Recognition*, Hawaii, June 1991.

[9] D. Geiger, A. Gupta, L.A. Costa, and J. Vlontzos. Dynamic programming for detecting, tracking, and matching deformable contours. *IEEE Transactions on Pattern Analysis and Machine Intelligence*, 17(3):294–302, March 1995.

[10] A. Guéziec and N. Ayache. Smoothing and matching of 3d curves. In *European Conference on Computer Vision*, Santa Margherita Ligure, Italy, May 1992.

[11] I.L. Herlin, I. Cohen, and S. Bouzidi. Detection and tracking of vortices on oceanographic images. In *SCIA'95*, 1995.

[12] I.L. Herlin, I. Cohen, and S. Bouzidi. Image processing for sequence of oceanographic images. In *Computer Graphics Technology for the Exploration of the Sea (CES'95)*, Mai 1995. Rostock.

[13] B. Horowitz and A. Pentland. Recovery of non-rigid motion and structure. In *Computer Vision and Pattern Recognition*, Hawaii, June 1991.

[14] M. Hospital, H. Yamada, T. Kasvand, and S. Umeyama. 3d curve based matching method using dynamic programming. In *International Conference on Computer Vision*, 1987.

[15] D. Metaxas and D. Terzopoulos. Shape and non-rigid motion estimation through physics-based synthesis. *IEEE Transactions on Pattern Analysis and Machine Intelligence*, 15(6):580–591, 1993.

[16] M. Okutomi and T. Kanade. A locally adaptative window for signal matching. *International Journal of Computer Vision*, 7(2):143–162, 1992.

[17] B. Serra and M. Berthod. Subpixel contour matching using continuous dynamic programming. In *Computer Vision and Pattern Recognition*, 1994.

[18] A. Szantai and M. Desbois. Construction of cloud trajectories to study the cloud life cycle. *Advanced Space Research*, 14(3):115–118, 1994.

[19] N. Ueda and K. Mase. Tracking moving contours using energy-minimizing elastic contour models. In *European Conference on Computer Vision*, Santa Margherita Ligure, Italy, May 1992.

[20] A. Yuille and P. Hallinan. Deformable templates. In Andrew Blake and Alan Yuille, editors, *Active Vision*. MIT Press, Cambridge, Mass, 1992.

Unité de recherche INRIA Lorraine, Technopôle de Nancy-Brabois, Campus scientifique,
615 rue du Jardin Botanique, BP 101, 54600 VILLERS LÈS NANCY
Unité de recherche INRIA Rennes, Irisa, Campus universitaire de Beaulieu, 35042 RENNES Cedex
Unité de recherche INRIA Rhône-Alpes, 46 avenue Félix Viallet, 38031 GRENOBLE Cedex 1
Unité de recherche INRIA Rocquencourt, Domaine de Voluceau, Rocquencourt, BP 105, 78153 LE CHESNAY Cedex
Unité de recherche INRIA Sophia-Antipolis, 2004 route des Lucioles, BP 93, 06902 SOPHIA-ANTIPOLIS Cedex

Éditeur

INRIA, Domaine de Voluceau, Rocquencourt, BP 105, 78153 LE CHESNAY Cedex (France)

ISSN 0249-6399